Deciphering Martian Flood Infiltration Processes at Hebrus Valles: Insights From Laboratory Experiments and Remote Sensing Observations

F. Costard, J a P Rodriguez, E. Godin, A. Séjourné, J S Kargel

JGR Planets

RESEARCH ARTICLE
10.1029/2023JE007770

Key Points:

- Hebrus Valles Mars shows fluvially dissected sinkholes, suggesting that enormous conduits served as megaflood subsurface evacuation routes
- We conducted a series of flume experiments to simulate infiltration patterns through sinkholes similar to those observed along Hebrus Valles
- We hypothesize the presence of discontinuities in the Martian subsurface due to subsurface drainage, forming organized conduits

Supporting Information:

Supporting Information may be found in the online version of this article.

Correspondence to:

F. Costard,
francois.costard@universite-paris-saclay.fr

Citation:

Costard, F., Rodriguez, J. A. P., Godin, E., Séjourné, A., & Kargel, J. S. (2024). Deciphering Martian flood infiltration processes at Hebrus Valles: Insights from laboratory experiments and remote sensing observations. *Journal of Geophysical Research: Planets*, *129*, e2023JE007770. https://doi.org/10.1029/2023JE007770

Received 25 JAN 2023
Accepted 28 DEC 2023

Author Contributions:

Conceptualization: F. Costard
Investigation: E. Godin, J. S. Kargel
Methodology: F. Costard, E. Godin
Supervision: F. Costard
Writing – original draft: F. Costard, E. Godin, A. Séjourné
Writing – review & editing: F. Costard, J. A. P. Rodriguez

Deciphering Martian Flood Infiltration Processes at Hebrus Valles: Insights From Laboratory Experiments and Remote Sensing Observations

F. Costard[1], J. A. P. Rodriguez[2], E. Godin[3], A. Séjourné[1], and J. S. Kargel[2]

[1]Université Paris-Saclay, CNRS, GEOPS, Orsay, France, [2]Planetary Science Institute, Tucson, AZ, USA, [3]Centre d'Études Nordiques, Université Laval, Québec, QC, Canada

Abstract In evaluating the unique geomorphology of Hebrus Valles on Mars, an outflow channel southeast of Utopia Planitia, we investigated the role of fluvial dynamics in forming subsurface conduits. Unlike typical Martian channels that terminate under younger sediment rocks, Hebrus Valles retains its downstream features, thus offering a window into surface and subsurface interactions between liquid water and regolith. Employing physical lab simulations, we utilized buried polygonal tunneling configurations in a sandy matrix to replicate the incision features observed at the channel's terminus. This study provides the first lab-based evidence demonstrating the role of conduits in conveying large floods in the Hebrus Valles. Our results lend support to the interpretation that Hebrus Valles conveyed high-volume floods by demonstrating that conduits are necessary to form the features observed on the surface of Hebrus Valles. The experiments also highlight the role of sinkholes as floodwater capture points, which suggests the formation of a regional interconnected network of subsurface channels and caverns. These findings affirm that fluvial dynamics in Hebrus Valles could have expanded subsurface discontinuities into functioning conduit systems, potentially directing floodwaters through an interconnected subterranean network.

Plain Language Summary Many channels on Mars end in areas hidden beneath younger layers in the northern plains. Hebrus Valles, southeast of Utopia Planitia, is unique because its lower parts are preserved as a mix of surface flows and underground pathways. Our investigation simulated the self-organization of surface-to-underground water flow via the formation of an underground network of channels. We performed experiments in the lab using tunnel-shaped structures in sand to copy the features found at the end of Hebrus Valles. This is the first lab evidence showing that surface features on Mars can be interpreted as having been formed by megafloods of water pouring into the ground in a reversal of outbursts of floods. Our experiments also show that sinkholes help connect different channels and caves in the area, which probably played a big part in helping floodwater "disappear" into the ground in Hebrus Valles.

1. Introduction

Over half a century, researchers have conducted extensive investigations of the Martian outflow channels (e.g., Baker, 1978, 1982; Baker et al., 1992; Mars Channel Working Group, 1983; Sharp & Malin, 1975; Warner et al., 2009). The Channeled Scabland on Earth serves as the most suitable analog for the Martian Outflow Channels (Baker, 1982, 2010), with abundant geologic evidence pointing to an origin from catastrophic floods (Bretz, 1923, 1969, 1982; Bretz et al., 1956; Pardee, 1942). Unlike the Channeled Scabland, which took shape through bedrock incision caused by glacial lake outburst floods, the Martian outflow channels likely formed as a result of groundwater outbreaks generating massive floods that reached the northern plains, eventually ponding into hypothetical northern ocean(s) (Baker et al., 1991; Clifford & Parker, 2001; Head et al., 1999; Parker et al., 1993).

Throughout the Late Hesperian Period, this/these ocean(s) likely led to the formation of extensive sedimentary deposits within the Vastitas Borealis Formation (VBF) (Barlow et al., 2000; Clifford & Parker, 2001; Costard & Kargel, 1995; Kreslavsky & Head, 2002; Mouginot et al., 2010). It was proposed that the VBF consists of catastrophic flood and marine sediments (Carr & Head, 2003; Clifford & Parker, 2001; Tanaka et al., 2005), and has undergone extensive resurfacing for approximately 3 billion years (Catling et al., 2012; Tanaka et al., 2014). After the hypothetical ocean(s) froze, the VBF might have preserved substantial ice volumes (Clifford & Parker, 2001; Mouginot et al., 2010; Séjourné et al., 2012; Stuurman et al., 2016). However, the lowermost reaches of these

outflow channels are concealed by the VBF (Tanaka et al., 2005). This concealment poses a challenge in studying the impact of Martian catastrophic floods on the landscape as they moved into the northern plains. A unique case is the Hephaestus Fossae and Hebrus Valles, located southeast of Utopia Planitia (20°N, 233°W). This outflow channel, stretching approximately 350 km from two distinct source pits, has lower areas that postdate the VBF's emplacement (Rodriguez et al., 2012; Tanaka et al., 2005) (Figure 1a). It was proposed that the source pits are outlets of groundwater bodies formed by the magmatic melting of an extensive layer of ground ice accumulation due to the presence of an internal volcanic activity (Leverington, 2011; Nerozzi et al., 2020; Rodriguez et al., 2012). Hephaestus Fossae is an orthogonal network of less than 2 km-wide channels. Hebrus Valles is an Early Amazonian outflow channel (Nerozzi et al., 2020) with 2–10 km-wide channels and fluvial bedforms (streamlined islands, fluvial terraces) that are features common to catastrophic flood erosion (e.g., Baker, 1978, 1982; Baker et al., 1992; Mars Channel Working Group, 1983; Sharp & Malin, 1975; Warner et al., 2009), suggesting an abrupt release of massive amounts of meltwater. However, the precise volume of the groundwater released remains undetermined.

Interestingly, Hebrus Valles features a fluvial terminus consisting of polygonal patterned networks of pits (Figure 1a) and troughs (Figure 1b) which are up to approximately 2.5 km across and around 0.5 km deep (Sharma et al., 2019). Evidence of Hebrus floods infiltrating into caves includes channels abruptly disappearing into a large cluster of pits and erosion zones cutting to the base of some pits and troughs (Figure 1c; Rodriguez et al., 2012). These infiltration zones likely consist of the VBF marginal deposits (Tanaka et al., 2005) of 100 m in thickness (Campbell et al., 2008). The presence of deeper groundwater during the Hesperian Period was previously suggested by a numerical model from Clifford (1993) and is supported by a 20 km diameter fluidized ejecta crater named Hephaestus crater overlapping Hebrus Valles (Figure 1b). Such rampart craters are mostly produced during the impact by the fluidization of a volatile rich subsurface layer of permafrost (Barlow et al., 2000; Tanaka, 1997). The depth of its excavation is estimated to be about 6 km (with a diameter/depth ratio of 3), indicating that the depth of the volatile rich layer must have significantly exceeded the VBF thickness. Recently, the Chinese Zhurong rover discovered fine-layered stratification of sediments and an indurated layer in southern Utopia Planitia, suggesting episodic ground water table fluctuations during the Late Hesperian to Early Amazonian period, precisely at Hebrus Valles' location (Hamran et al., 2022).

The regional VBF area features cones, mounds and pits, which are interpreted as Martian analogs to terrestrial mud volcanoes (Rodriguez et al., 2012; Skinner & Mazzini, 2009; Tanaka, 1997; Tanaka et al., 2003). Numerous cones align with the margins of giant polygons. These polygons with diameters of several kilometers and troughs ranging from 5 to 115 m deep (Buczkowski & McGill, 2002; Hiesinger & Head, 2000) encircle the Utopia basin (Buczkowski et al., 2012; Hiesinger & Head, 2000; McGill & Hills, 1992). In southern Utopia, the polygons are 5–20 km in diameter, irregularly shaped, and occasionally not fully enclosed (Buczkowski et al., 2012; Hiesinger & Head, 2000). Their formation could result from tectonic deformation (Mutch et al., 1977) or desiccation or compaction of previously water-rich sediments (Buczkowski et al., 2012; McGill & Hills, 1992; Pechmann, 1980). The interaction of permafrost and intrusive magmatism has also been suggested to explain the tectonic deformation (Rodriguez et al., 2003) with thermal cooling and contraction of the permafrost (Carr & Schaber, 1977).

The origins of Martian outflow channels have sparked considerable debate. Some analog studies have been proposed, with the most renowned being the Channeled Scablands (Bretz, 1969, 1982), which account for the bedform and fluvial dynamic of catastrophic floods on Mars. Costard et al. (2007) also suggested a Siberian analog between the Lena River and Martian outflow channels, as both hydrological systems were or are associated with a periglacial environment characterized by deep and continuous permafrost. The unique morphology of Hebrus Valles characterized by interconnecting caves and sinkholes strongly suggests a volatile-rich subsurface in the past, as sinkholes and connecting conduit ceilings are commonly found in terrestrial permafrost environments (Costard et al., 2016).

In the Canadian Arctic of Bylot Island, snowmelt runoff that concentrates into streams over ice-rich permafrost can initiate some internal tunneling (Fortier et al., 2007), leading to extensive networks of gullies and underground flows (Figure 2). Within the confines of the C-79 glacier valley situated on Bylot Island, locally referred to as the Qalikturvik valley (Nunavut, Canada), the aftermath of snowmelt results in the aggregation of runoff into distinguishable streams across a syngenetic ice-wedge polygon terrace (Figure 2). Annual snowmelt runoff triggers a sequence of internal tunnel formation via the exploitation of pre-existing crevices and sinkholes, consequently inducing gullying within the ice-rich permafrost through a process of fluvial thermal erosion, which occurs primarily along the extensively structured vertical ice wedges (Fortier et al., 2007).

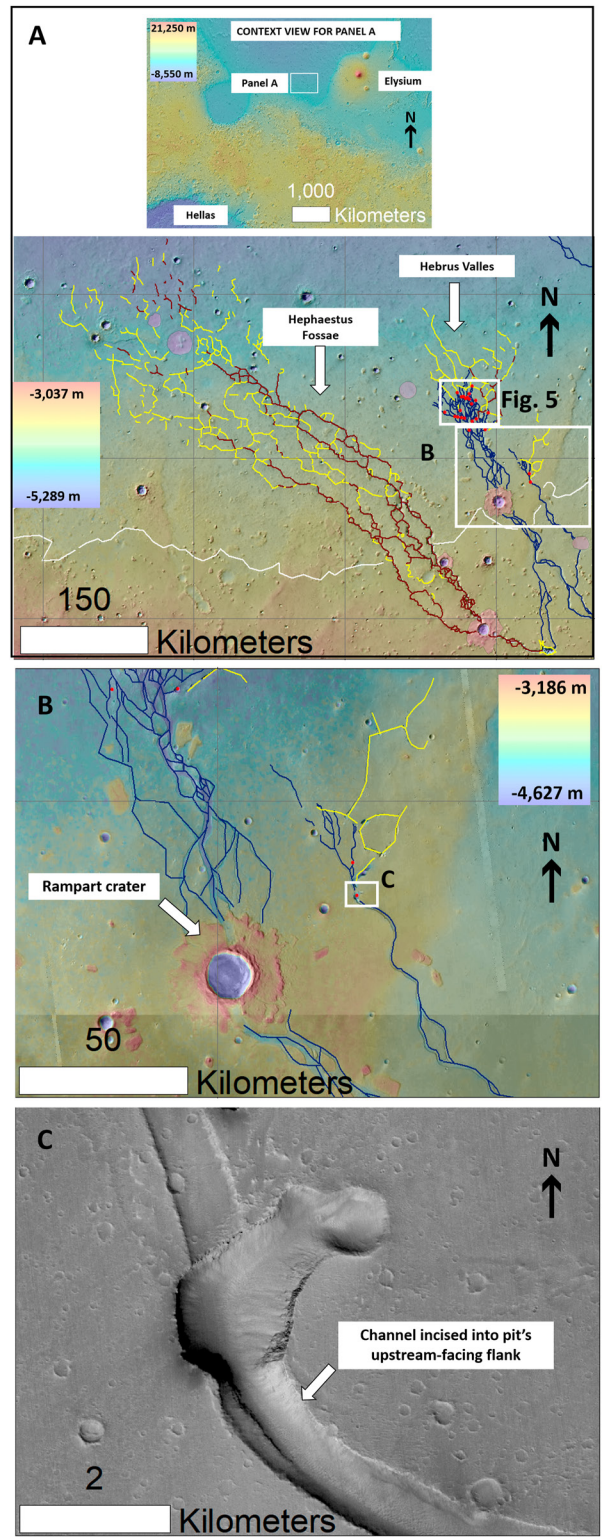

Figure 1. (a) Hebrus Valles displays sinuous valleys over the floodplain, corresponding to the outflow classification. However, the presence of orthogonal networks and caves suggests additional scenarios. Red lines represent troughs, blue lines indicate outflow channels, yellow lines show patterned networks of troughs, and red dots mark single pits and caves. The location was centered at 20°N, 125°E. Image courtesy of NASA and USGS. Scale: 680 km × 400 km. (b) Hephaestus crater. A 20 km rampart crater implies the presence of a volatile-rich subsurface in the past at a depth just underneath the Hebrus Valles channels. Image credit: HRSC, Mars Express, ESA/DLR/FU Berlin (G. Neukum). (c) Close-up of a pit, formerly interpreted as a sinkhole with an upstream margin eroded and leveled to its base as the flow transitioned into subterranean conduits. HRSC ID: H9490_0000_ND3. Location: 22°12′N, 125°16′E. Image credit: ESA/DLR/FU Berlin.

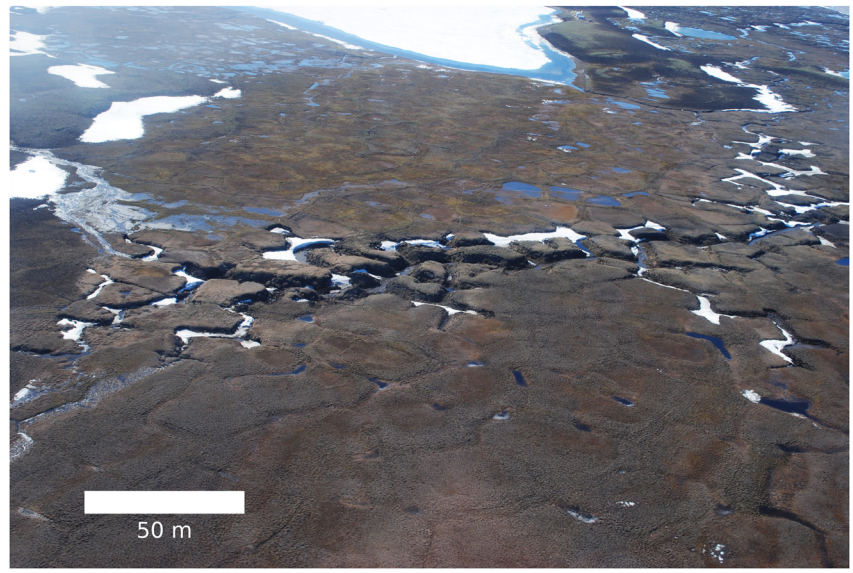

Figure 2. Internal tunnel and sinkhole formation on Bylot Island, Nunavut, Canada. The polygons manifest themselves with diameters ranging between 10 and 15 m, providing a measure of scale. Image credits: E. Godin and D. Fortier. Location: 73.15°N latitude, −79.94°E longitude.

Geological studies (Rodriguez et al., 2012), terrestrial analogs (Godin & Fortier, 2012; Godin et al., 2014), and features present in Hebrus Valles suggest that large floods may have interacted with subsurface conduits; however, the nature of this interaction is currently unknown. Our study aims to investigate the possibility that the flows forming Hebrus Valles were connected with preexisting underground cavernous networks. We present the first laboratory-scale simulation of outflow channel floods propagating over shallow cave systems, as proposed for Hebrus Valles.

2. Methods

We conducted mapping of channels, pits and craters in remote sensing imagery of Hebrus Valles and ran a series of laboratory experiments to observe the conduit excavation process, in order to investigate whether the presence of conduits leads to the formation of the types of features observed on the Martian surface.

2.1. Remote Sensing

Raw spacecraft data used in this study include HiRISE (McEwen, 2007), CTX (Malin, 2007), and MOLA data (Neumann et al., 2003) archived in NASA's Planetary Data System as well as HRSC data archived by ESA (European Space Agency, 2020) (Figure S1 in Supporting Information S1). The images were calibrated and georeferenced using ArcGIS® software (ESRI, 2021). Remote sensing data were subsequently combined and measurements were taken to analyze the morphology of the channels and caves in Hebrus Valles. Topographic data and volumetric estimations have been derived using digital elevation models (DEMs) from Mars Orbiter Laser Altimeter (MOLA) at 460 m/pixel horizontal and 1 m vertical resolutions (Rodriguez et al., 2012). We identified several fluvial type bedforms along Hebrus Valles, such as wide and flat channels, terrace-like benches along edges of streamlined hills and plateaus, and streamlined islands with downstream tails. We classified isolated pits that are circular to elongated sinkholes with accurate and well-defined rim. We also mapped structurally patterned networks of troughs with rectilinear geometries, mostly along Hephaestus Fossae.

Additionally, we used HRSC images (10 m/pixel, Jaumann et al., 2007) from the Mars Express mission (ESA, DLR) to map the area and to classify and measure features such as channels and pits (Figure 1).

2.2. Large-Scale Flume Experiments

2.2.1. Overview

To investigate whether the landscapes in terminal Hebrus Valles were formed due to infiltration, we conducted five experiments simulating a cavernous underground system with an over-flooding scenario. Our experiments

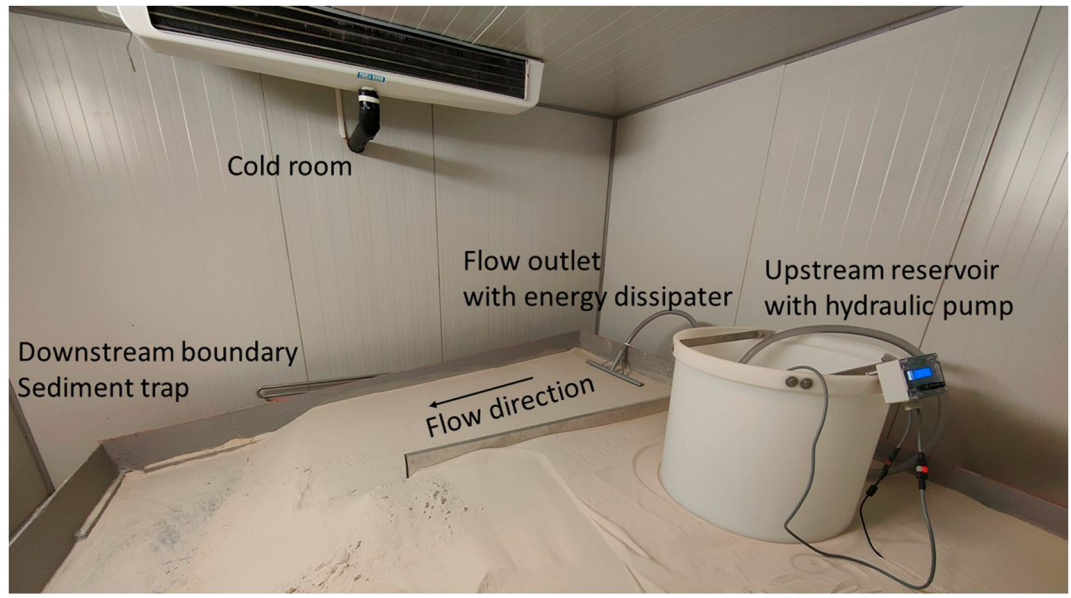

Figure 3. Oblique view of the experimental setup showing the water inlet and outlet.

aimed to better understand how floods are captured by sinkholes and can lead to a regional interconnection of channels and caves in the Hebrus Valles. To replicate the Hebrus morphology, we constructed an orthogonal pattern of ice slabs before the experimentation, which after melting simulated cave geometries. We then performed a series of five physical modeling experiments of infiltration (Exp 1 to Exp 5, Figures S2–S6 in Supporting Information S1) of overland flow into subsurface conduits, which facilitated the incision of channels. Exp. 1 to 3 were conducted with unfrozen sediments and Exp. 4 and 5 were performed using frozen sediments. We also ran a control experiment in which subsurface conduits were not present (Exp 6, Figure 8).

2.2.2. Experimental Setup

We placed the entire experimental setup in a cold room at −5°C to control the formation of artificial tunnels (Figure 3). The flume experiment consisted of a 2 m × 1 m rectangular box with a sediment thickness up to 0.2 m (Costard et al., 2021). The base slope of the rectangular box was set at 3° to release excess water during each experiment. We used an upstream reservoir connected to a hydraulic pump to control the discharge during each experiment. The flow outlet included an energy dissipater installed upstream over the sediment bed. At the downstream boundary, the flow outlet featured a sediment trap and a pump was installed to capture water and sediments after flooding (Figure 3). The channel bed incorporated vertical ice slabs arranged into interconnected polygons, which upon melting left behind identically polygonal underground conduit systems (Figure 4; Figure S7 in Supporting Information S1). We justified this orthogonal network due to the presence of giant polygonal patterns at the termini of Hebrus Valles.

The primary challenge in conducting the experiments was to prepare a homogeneous porous medium saturated with water to ensure repeatability. Consequently, we avoided silty clay materials due to difficulties in maintaining homogeneity and controlling the porous media's rheology. Instead, we chose fine quartz crystals sand (SiO_2) with a proportion exceeding 99.7%. Granulometry ranged from 100 to 800 µm with a D_{50} of 200 µm. Sibelco (https://www.sibelco.com/materials/silica) supplied the clean and well-calibrated sand sourced from Fontainebleau quarries southeast of Paris.

We employed a well-established technique for creating a homogeneous saturated soil medium (Costard et al., 2021). To achieve optimal porosity, we combined sand with water to obtain a wet density of 1.81 g.cm^{-3} corresponding to the "Proctor compaction" technique (Costard et al., 2021). We progressively mixed the dry sand with water until the pore space was saturated. Then, we compacted 5 cm layers manually and stacked them to reach a 0.2 m thickness. This method facilitated parametric control over a homogeneous pre-saturated block weighing approximately 0.5 tons with an 18% volumetric water content.

Before each experiment (Exp. 1 to Exp. 5), we constructed the cavernous underground system as follows: (a) Before starting the cold room at −5°C, we formed an ice wedge network (Figure S7 in Supporting Information S1)

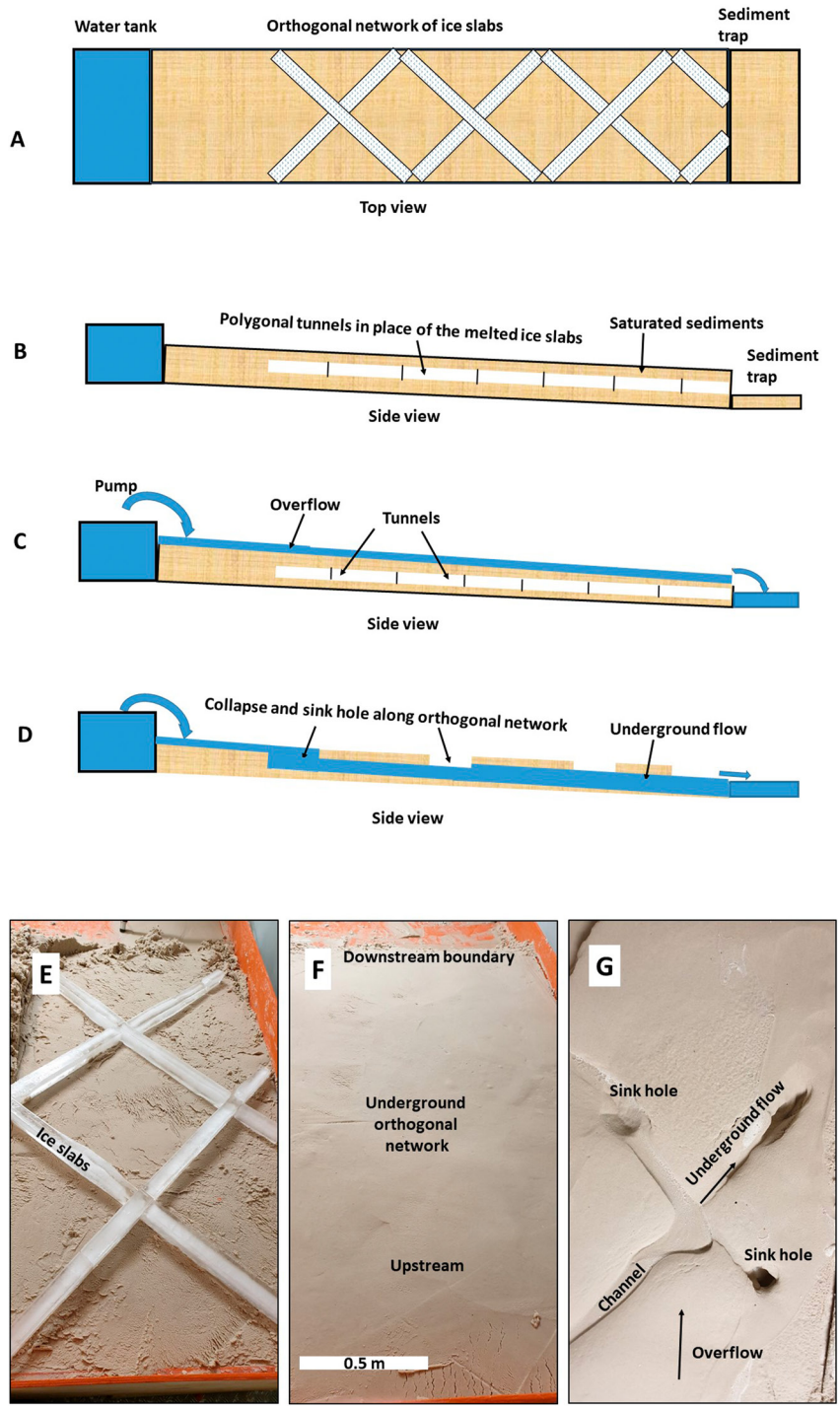

Figure 4. Schematic diagrams (a–d) that collectively detail the stages of the experimental setup. (a) Plan view of an orthogonal network of ice slabs situated within a matrix of saturated sediments. (b) Cross-section perspective depicting the orthogonal troughs which emerge following the melting of the ice slabs. (c) Side view of an overflow event characterized by water infiltration. (d) Subsequent sinkhole formation along the orthogonal matrix and obliteration by sedimentation of the conduit. (e) Experiment in the cold room showing an artificial orthogonal network of ice slabs overlying a layer of saturated sandy material. (f) The orthogonal network of ice slabs is filled with water-saturated sediments and then frozen at −5°C. (g) After a warming phase at +17°C, the ice of the artificial polygonal network preferentially melts with the formation of tunnels. Here, the troughs and pits are observed after an overflooding of 4 min.

Table 1
Results From Various Fluvial Erosion Experiments (Vertical Incision Within Cave Formation) Conducted With Saturated Sand Differing Ground Temperatures and Discharge Rates

	Exp. 1	Exp. 2	Exp. 3	Exp. 4	Exp. 5	Exp. 6
Discharge (mL.s^{-1})	90	18	45	**45**	**90**	45
T soil (°C)	+17	+17	+17	**−5**	**−5**	+17
T water (°C)	+17	+17	+17	**+17**	**+17**	+17
Max. depth main channel (mm)	12	5	5	**4**	**4**	2
Max. width main channel (mm)	350	150	200	**180**	**120**	55
Max. depth main pit (mm)	26	20	22	**10**	**22**	N/A
Max. diameter main pit (mm)	220	110	120	**66**	**110**	N/A

Note. Color and bold values represents frozen sediment configurations. Exp. 6 was performed without polygonal underground conduit system.

with individual ice slabs measuring 5 cm by 5 and 50 cm in length to simulate the polygonal troughs at terminal Hebrus Valles (Figure 1) and at Bylot island (Figure 2). (b) We introduced wet (saturated) sand, burying the ice wedges beneath a 10 cm thick sediment layer. (c) Then, we subsequently cooled down the assembly (ice slabs and saturated sand) to −5°C. (d) After complete freezing, we warmed up the cold room to +17°C, to cause ice to melt within the artificial polygonal network, forming tunnels. For the experiments 1 to 5, the icy orthogonal grid was present but all the ice melted away during the warming phase. The surrounding ground ice in the saturated sediment melted without surface deformation due to 18% water saturation (Figure 4e). Despite ice melting in the polygons and sand, the former presence of polygonal ice slabs generated a polygonal void structure within the thawed system (Figure 4b). During the warming phase and before the flow episode, sand did not flow into the space left by the ice wedges and this structure governed surface drainage and subsurface erosion due to channelized surface flow. (e) Although the final surface remained flat, the system developed polygonal troughs in place of the ice wedges (Figure 4). Finally, we maintained the sand surface at a positive temperature of +17°C for exp. 1–3 or cooled it down to −5°C again for exp. 4 and 5. In order to control if underground conduits are necessary for erosion and pit formation, we also performed a conduit- free experiment (Exp. 6) in which subsurface conduits were not present (Figure 8).

2.2.3. Initial and Boundary Conditions

We set a polygonal tunnel network under the initial condition, with a flat bed of saturated sediments as the initial surface morphology. We used an external reservoir connected to a hydraulic pump (Orca 500) with a K500 digital flow controller (from Emriver, Inc) to simulate flow, precisely measuring flow rates between 18 and 210 mL.s^{-1}. We conducted five experiments (Exp. 1 to Exp. 5, Figures S2–S6 in Supporting Information S1), varying discharge and soil temperature. For these experiments, the flow outlet was attached to the upstream end of the box (Figure 3) with constant inlet discharges for a given run of 18, 45, and 90 mL.s^{-1} and sediment temperatures of −5°C and 17°C. The temperature of the sediment was measured using some platinum temperature sensors (accuracy 0.1°C) inserted in the 200 mm of sediment at a depth ranging from 5 mm beneath the soil interface to 200 mm depth.

Due to the scale of the experimental setup (0.5 ton of wet sand), the basal slope angle was fixed. We ran experiments until complete obliteration of pits by sedimentation. An additional experiment (Exp. 6, Figure 8) used homogeneous sediment without tunneling.

We derived individual frames from time-lapse photography to chart the temporal evolution of sinkhole formation. The morphometric attributes of the resultant pits post-flooding as well as the timescales associated with their formation and obliteration were quantified utilizing a depth gauge micrometer and a digital Vernier caliper (Table 1). Laser scanning was precluded due to issues with water reflection during flooding events.

Although the uniform tunnel size and granular structure within the soil do represent a simplification of the natural setting, the primary aim of these experiments was to assess the role of conduits in facilitating underground flow. The experiments were conducted for sediments representing a range of erodibilities, with unfrozen saturated soil representing easily erodible sediments (Experiments 1–3, Figures S2–S4 in Supporting Information S1) and

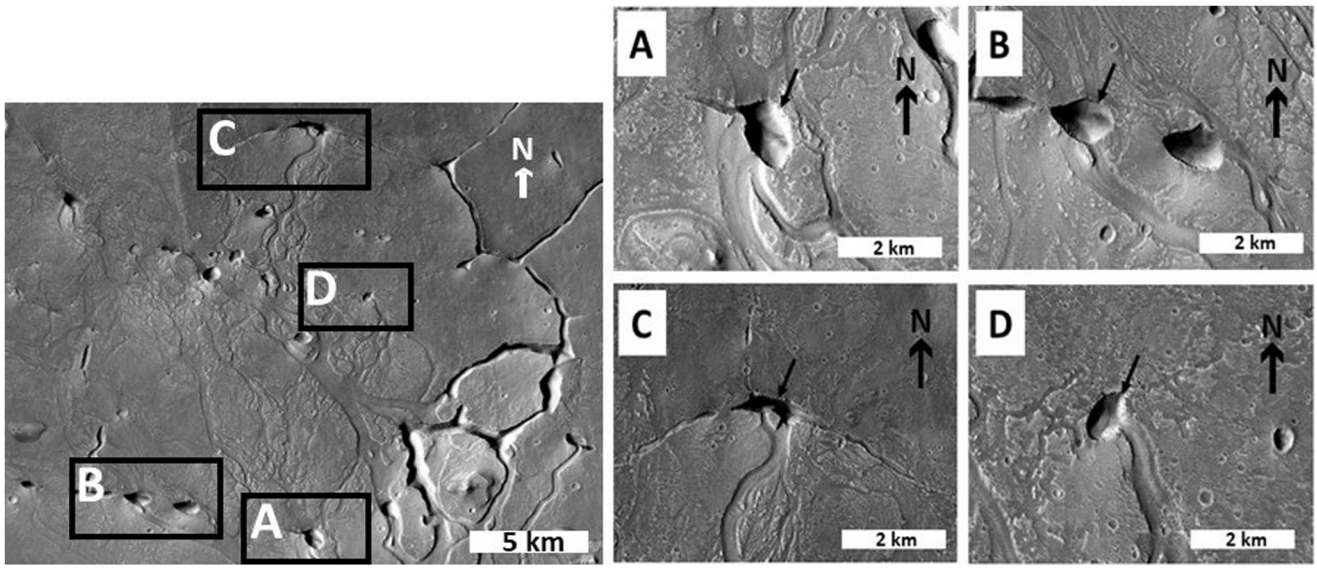

Figure 5. The Figure illustrates a comparative analysis of cave formations in Hebrus Valles, Mars. See the context image on the left for location and on Figure 1A. Images A and B depict isolated sinkholes (black arrows) disconnected from the main channel. Images C and D provide detailed insights into sinkholes, resulting in an extensive underground cavernous system via a collapse process. The valley flow from the bottom to the top of the image terminates conspicuously at a cave (black arrows). Image credit: HRSC, Mars Express, ESA/DLR/FU Berlin (G. Neukum). (a) HRSC ID: H5140_0000_ND3, location: 21°.38'N, 125°39''E. (b) HRSC ID: H5122_0000_ND3, location: 21°44'N, 125°19°E. (c) HRSC ID: HB599_0000_ND3, location: 22°19'N, 125°31'E and (d) HRSC: ID: H5140_0000_ND3, location: 22°03'N, 125°37'E.

frozen saturated soil representing less erodible sediments (Experiments 4–5, Figures S5 and S6 in Supporting Information S1).

3. Results

3.1. Results From the Survey of Remote Sensing Images

In the Hebrus Valles, large troughs might represent collapsed conduits formed by subsurface sediment evacuation (Rodriguez et al., 2012) along extensive polygonal networks. These expansive caves enable flood (and sediment) infiltration beneath the surface. The water entered the caves without reemerging (at the imagery scale). The northern limit of Hebrus Valles displays 22 isolated pits and trough networks (Figure 1), suggesting the drainage of floodwaters into the subsurface (Rodriguez et al., 2012). We identified fluvial type bedforms (islands, terraces) and kilometer scale channels of Hebrus Valles suggesting drainage of floodwaters and local channel incisions with caves.

From our GIS mapping (Figure 1), two types of caves are observed along Hebrus Valles: (a) 13 caves closely connected to channels, exhibiting scarp retreat, and, (b) 9 caves without an apparent connection to overland flows, instead being groundwater-supplied by an underground cavernous system (Figure 5). Figures 5a and 5b show the geographic relation of isolated pits located in the middle of the main channel. These sinkholes are disconnected from the main channel and are formed after flooding episodes. Figures 5c and 5d show isolated pits located at the terminal part of the main channel. The channels abruptly stop at the sinkhole. Images C and D provide detailed insights into sinkholes that formed during the flood sequence, resulting in an extensive underground cavernous system via a collapse process. The valley flow from the bottom to the top of the image and conspicuously terminates at a cave, indicating a likely connection between the sinkhole and the underlying cavernous structure.

3.2. Experimental Results

Our flume provides large floods with the formation of typical fluvial bedforms (wide and flat channels without tributaries) similar to those of Martian outflow channels. The development of interconnected tunneling and caves within the soil after subsequent flooding from the upstream section of the experiment is illustrated in

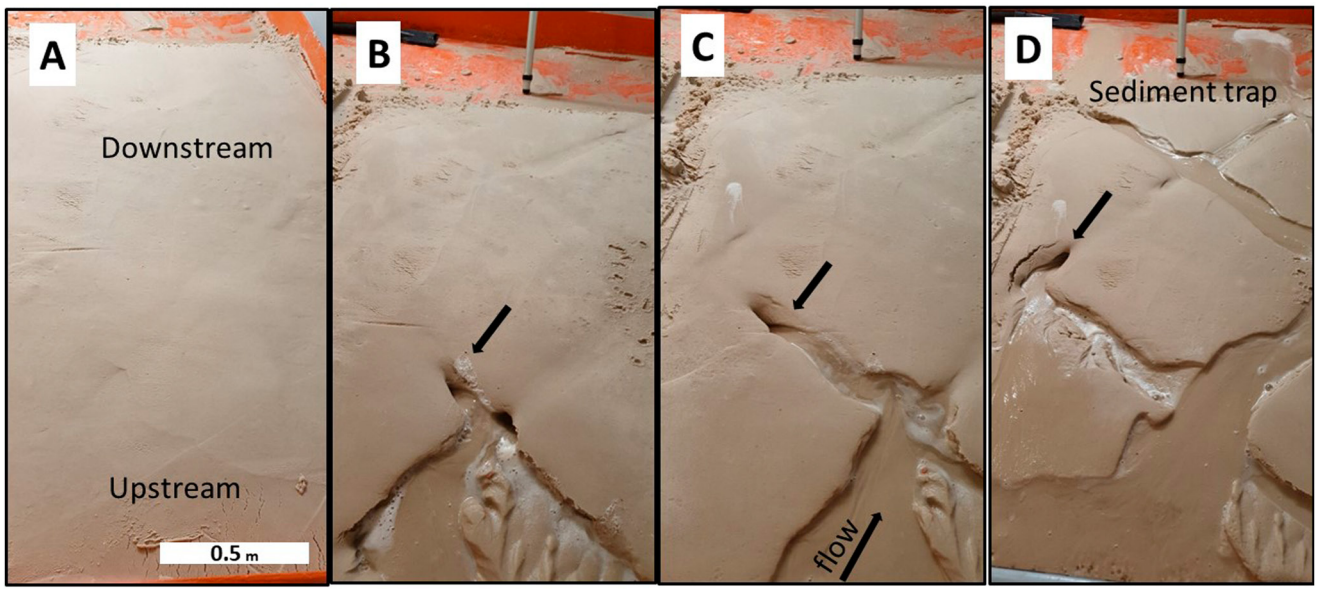

Figure 6. Evolution of an orthogonal network illustrating the formation of tunnels and caves (Exp. 2). Images are captured at 2-min intervals from left to right. Scale: 1 m × 2 m. (a) Initial stage with no flow. (b) $t + 2$ min: the collapse of overlying layers and sinkhole formation (Phase 1). (c) $t + 4$ min: internal tunneling phase. (d) $t + 6$ min, a new cave emerges (black arrow) where channels are captured by a newly formed cavity.

Figure 6. That experiment provides detailed insight into the various stages of collapse formation. The observed general patterns are common to all the experimental scenarios except Exp. 6. In the experiment's initial stage, flow concentrated in one channel with flow depths ranging from 2 to 8 mm (Figure 6b). At $t + 2$ min, floods generated by the upstream pump were captured by the collapsed cavern (Figure 6b), creating a sinkhole. The channel abruptly ends at the cave (black arrow), indicating a connection between the sinkhole and an underground cavernous system. At $t + 6$ min, subsidence occurred along the elongated cavity, accompanied by an underground cavernous flow and the development of new orthogonal channels, leading to another collapse (black arrow in Figure 6c).

At the initial stage, the surface appears relatively smooth, but an artificial orthogonal network of tunnels exists beneath (Figure 6a). Figure 6b shows the subsequent collapse of the overlapping layers after water infiltration. At $t + 2$ min, upstream water flow erodes the sediment through a vertical incision (Figure 6b) with a collapse of overlying layers, a channel incision, and a sinkhole formation (refer to Table 1). At $t + 4$ min, overland flow traverses the underground tunnel, eventually connecting to a new orthogonal network of tunnels (marked by a black arrow). The flow then reaches the underground conduits (Figure 6c), stabilizing the vertical incision after 4 min. During the internal tunneling phase, subsequent collapses create a new depth of 20 mm (Figure 6c). During that internal tunneling phase, subsequent collapses form pits as deep as 20 mm, but only after 6 min of flooding. The final stage involves channel incision being captured by the subsurface, resulting in the formation of new sinkholes (Figure 6d).

As the discharge increases from its lowest to highest value, the maximum channel depth after 4 min increases from about 5 mm to over 20 mm. The higher discharge results in deeper and larger channels and pits. A discharge of 18 $mL.s^{-1}$ yields a channel incision of 5 mm, and a discharge of 90 $mL.s^{-1}$ results in a maximum channel erosion of 12 mm (Figure 7 and Table 1). Rapid erosion leads to a high sediment load in the channel, obliterating some previous caves (Figures S2–S4 in Supporting Information S1). Upon completing each experiment (Experiments 1 to 3 for unfrozen sediments), we observed a reduction in pit depth caused by sediment accumulation, which obliterates the conduit within the pit (Figure 7).

We also conducted experiments involving frozen sediments (Experiments 4 and 5) to test the influence of erodibility (Figures S5 and S6 in Supporting Information S1). The same dynamic and morphological evolution were observed, but with reduced vertical erosion (Figure 7).

In a control experiment (Experiment 6, Figure 8) without subsurface conduits, the results show a lack of erosional features, instead presenting small-scale fluvial braided channels distributed homogeneously across the flat

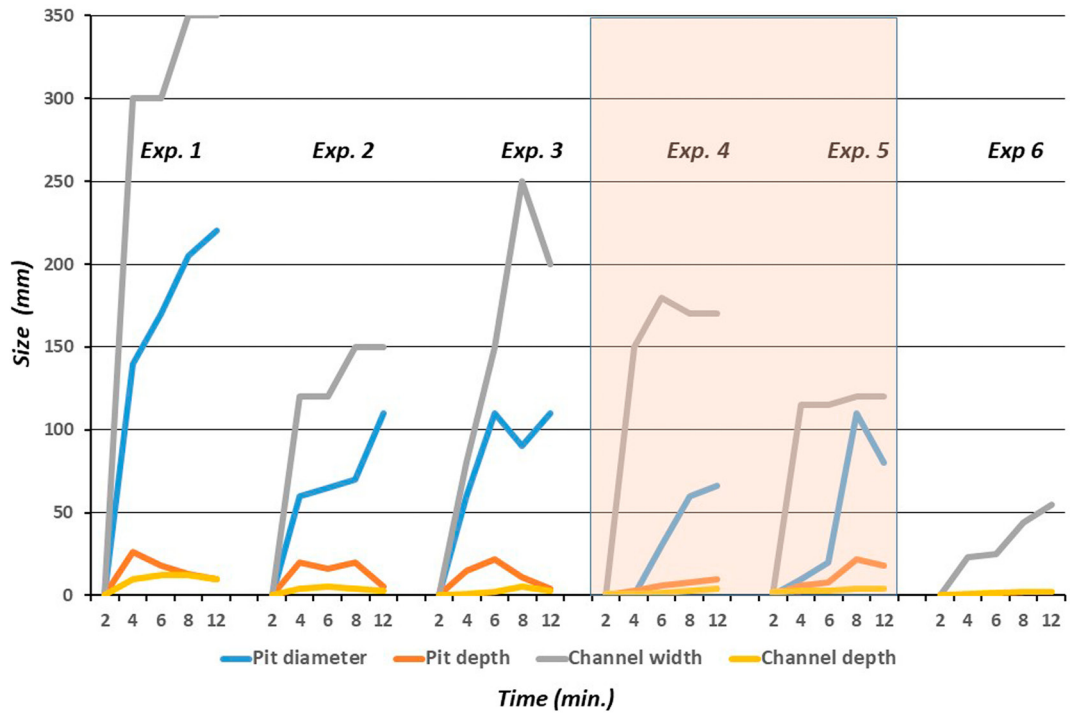

Figure 7. This time series, acquired every 2 min, displays the morphological evolution of channels and pits across five experiments (refer to Table 1 for characteristics) with subsurface conduits. Depth and width measurements were derived from time-lapse imagery (see Figures S2–S6 in Supporting Information S1). The pink color represents the frozen sediment configuration.

surface of saturated sediments without any pits or sinkholes. Conversely, Experiments 1 to 5 with subsurface conduits promote incision and concentration of flows toward pits and sinkholes (Figures S2–S6 in Supporting Information S1).

4. Discussion

4.1. Insights From Mars Studies

Multiple studies have uncovered cavernous systems on Mars (Rodriguez et al., 2003, 2012) with potential existing sinkholes (Sulcanese et al., 2018). Researchers have proposed episodic underground drainage along conduits for outflow channels (Rodriguez et al., 2015) and small-sized thermal contraction polygons in Utopia Planitia, which exhibit diameters of several tens of meters and display collapse patterns and morphologies of disconnected sinuous elongated pits along polygon cracks (Costard et al., 2016). The Hebrus outflow channels possess a considerable cumulative volume estimated at 206 km³, a figure that notably surpasses that of the terminal trough networks (Figure 1), which register volumes of merely 6.5 and 8.8 km³, respectively (Rodriguez et al., 2012). This differential signifies a disparity of two orders of magnitude and infers that the trough networks could primarily be remnants of more expansive cavern networks that have experienced collapse (Rodriguez et al., 2012). This hypothesis gains further credibility from observations of fluvial features which terminate in subsurface pits that lack visible exit points (Figure 1c), suggesting the potential existence of larger and concealed cave systems.

The presence of orthogonal networks and caves, which locally collapse into giant polygonal patterns (Figure 1), suggests flood infiltration at the terminus of Hebrus Valles. The absence of terminal deposits (e.g., fans) at the network's end remains unexplained. One possibility involves floods eroding channels with substantial eroded sediments; however, water flow infiltration into caverns was too slow, resulting in gradual sediment accumulation in large-scale underground cavity networks.

Rodriguez et al. (2012) proposed a morphogenetic connection between channels and sinkhole presence. A sedimentary evacuation from within indurated permafrost was suggested to explain the possible clustering of mud

Figure 8. Braided channel formation in a control experiment in which subsurface conduits are not present (Exp.6, Table 1).

volcanoes. Lava tubes, common conduits in volcanic environments, have been documented near Elysium volcanoes (Sauro et al., 2020). Consequently, it is plausible that the VBF's subsurface could include some (Catling et al., 2012).

4.2. Insights From Arctic Analogs

The presence of subsurface conduits is a relatively common process in an analogous arctic environment. Examinations of Bylot Island from previous field studies (Godin & Fortier, 2012; Godin et al., 2014) show that surface flow can infiltrate open cracks and sinkholes within ice-wedge polygonal systems, consequently forming and enlarging tunnels via fluvial thermal erosion. This recurring phenomenon may stabilize when water flow diminishes and refreezes inside the tunnel. Meter-scale tunnels, which intersect newly exposed ice wedges horizontally, have been detected containing an upper layer of thermokarst cave ice from surface water, which overlays a combination of frozen coarse-sized sediments such as sand, gravel, and peat (Godin & Fortier, 2012; Godin et al., 2014). Under these circumstances, tunnels (Figure 9a) are fairly prevalent. Moreover, the onset of tunneling activates various positive feedback mechanisms including improved local drainage and stream piracy, which contribute additional heat to the system (Figure 9b), thus amplifying the erosion process. The gully head area, characterized by sinkholes, has been observed to rapidly recede during the brief summer season: hundreds of meters in the first year of active gullying and subsequently ranging from tens of meters to 100 m subsequently. In the early stages of a flood, complete sets of polygons may be removed when their ceiling collapse, leading to the formation of broad channels (tens of meters wide) afterward. That arctic analog shows some similarities with our flume experiment,

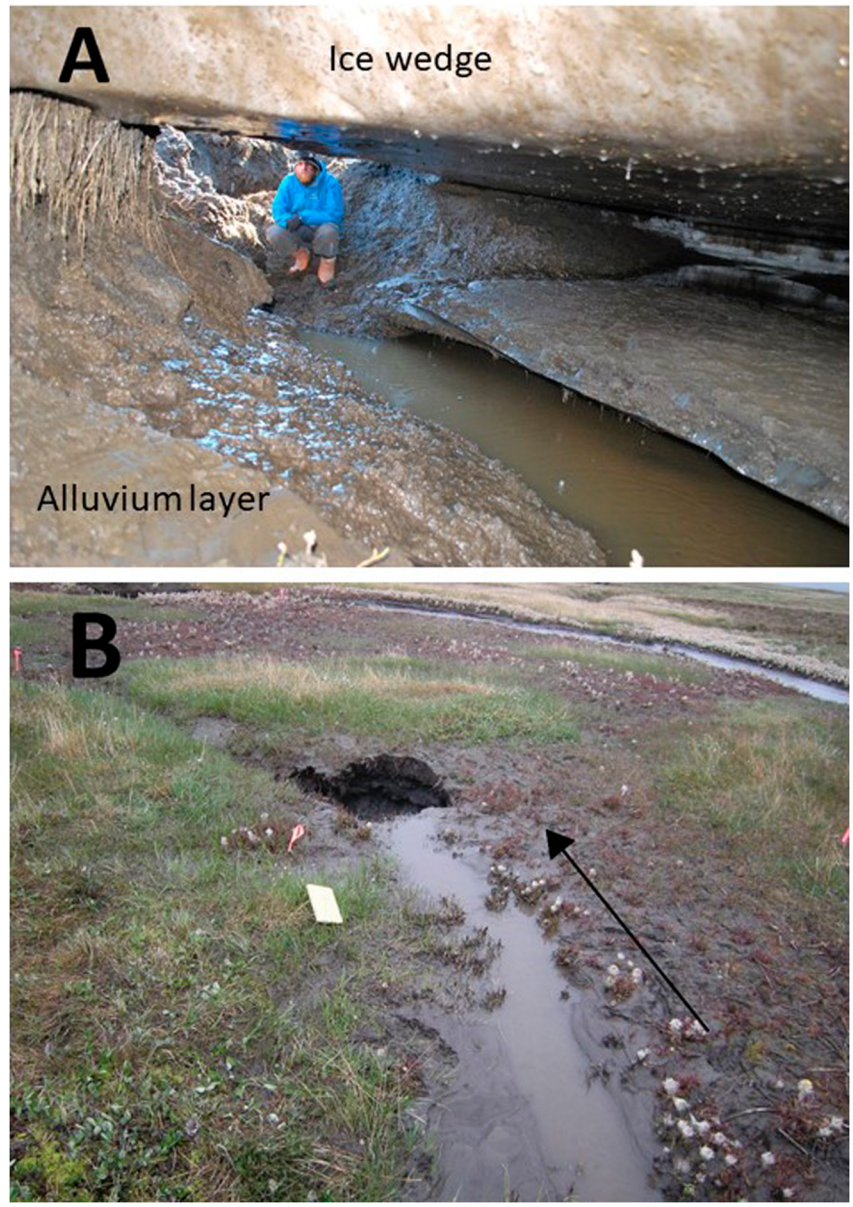

Figure 9. Thermal erosion tunnel in Qalikturvik Valley. (a) Interior view of the thermal erosion tunnel with a person for scale, revealing how an ice-wedge polygon junction was truncated due to an inflow of underground water from an upstream sinkhole. The tunnel floor exhibits an alluvium layer overlying the permafrost, while the ceiling is supported by an ice-wedge (73.156°N, −79.944°E). (b) Sinkhole draining an adjacent stream, with a white logbook located to the left of the stream serving as a scale reference (73.155°N, −79.945°E). Black arrow: flow direction. Photo credits: E. Godin and D. Fortier.

like subsurface conduits, but also some differences with Hebrus Valles on Mars, like the presence in the Arctic of sediments either transported downstream or deposited on the newly established channel floor.

4.3. Insights From Laboratory Simulations

Our experiment supports high-volume fluvial events in Hebrus Valles with the formation of typical wide and flat channels similar to those of Martian outflow channels. This study lends support to the interpretation that Hebrus Valles conveyed high-volume floods by demonstrating that conduits are necessary to form the features observed on the surface of Hebrus Valles. The erosion produced by a big flood flowing through the flume containing conduits produces the types of features we see in Hebrus Valles. Our experimental setup successfully replicated

orthogonal intersections and collapses found in the Hebrus Valles hydrographic network (Figure 6). Our experiment was limited by scaling issues (flume vs. Mars), does not serve as a direct scale analog of morphological landforms. As a result, its relevance extends to a specific process: examining the initiation and various interaction phases between an overflow and a cavernous system. The lab results reveal landscape development consistent with the interpreted event sequence inferred from Martian features at Hebrus Valles (Figure 1) and Bylot Island (Figure 2). Crucial evidence supporting the role of caves comes from our lab simulations (Figure 6), which display channel incision, tunnel subsidence, and sinkhole formation not observed in the conduit-free control experiment (Figure 7). Noteworthy is the observation of overlying layer collapse events (Figure 6d), reminiscent of the pit morphologies seen on Bylot Island (as illustrated in Figure 9b).

Our laboratory simulations (Exp. 1 to 5) shows that channel initiation (with widths between 120 and 350 mm and flow depths between 2 and 8 mm, see Table 1) quickly become coupled with underground drainage, resulting in localized collapses along the underground conduits (Figure 6d). The flow (from bottom to top in the images) primarily follows the cavernous underground system, with characteristic collapses developing due to the subsurface drainage of captured floods.

Experiments with frozen sediments (Exp. 4 and 5, Figures S5 and S6 in Supporting Information S1) show that the conduit from the pit remained sediment-free, explaining the relatively high pit depth value after 12 min of the experiment (Figure 7 and Table 1). Our experiments with frozen sediments (Exp. 4 and 5) demonstrate that the formation of sinkholes is possible along polygons or fractured terrains like those on Bylot Island (Figures 2 and 6) for a range of erodibilities, albeit with less efficient erosion than in cases with unfrozen sediments due to the frozen material's strength and the impact of latent heat (see Table 1; Figures S5 and S6 in Supporting Information S1).

The most suitable Mars analogs are observed with high-porosity unfrozen sediments, which promote both erosion and infiltration of flow during floods. A thin layer of sandy material overlying a layer with cavernous tunneling is necessary to reproduce the morphology of Hebrus Valles channels and the dynamic interaction between sinkholes and flows in Hebrus Valles. Contrarily, the conduit-free experiment (exp. 6, Figure 8) does not show any pits or sinkholes. Applying our experiments to Hebrus Valles, collapses tend to occur preferentially along zones of weakness, resulting in the formation of elongated pits and caves. These scenarios can account for the presence of collapses (Rodriguez et al., 2012) along caves, which predominantly form during flood episodes followed by extensive erosion and collapse of the underlying layers.

The laboratory experiments demonstrate that infiltration through subsurface discontinuities can produce features similar to those found on Mars. In both environments (frozen and unfrozen sand), our simulations reveal that floods rapidly become coupled with subsurface ground drainage through underground conduits. Figure 10 presents a dichotomy between controlled laboratory simulation and the geophysical reality of Martian terrains. Figure 10a illustrates the outcome of Exp. 1. Noticeable features include active sinkholes functioning as ingress points, facilitating the capture of fluid ingress into vacuous subterranean chambers. Figure 10b, on the other hand, depicts an analogous real-world manifestation on Mars, particularly in the Hebrus Valles region. In Hebrus Valles, fluvial dynamics likely resulted in floodwater being directed into subsurface reservoirs through sinkholes via a geomorphologic collapse process. Our laboratory simulation suggests a morphological concordance along the Hebrus Valles, where natural initial cavernous structures likely serve as preferential subsurface conduits, channeling fluid-sediment mixtures into these evacuated cavities.

Baker et al. (1991) suggested that floods from outflow channels onto Mars' northern plains created an immense body of water during the Hesperian Period, supported by evidence from Lucchitta et al. (1986) and Parker et al. (1989, 1993). The hypothesis posits that these outbursts coincided with CO_2 release, causing temporary greenhouse warming. Methane, however, would be more effective than CO_2 in this regard (Kasting & Brown, 1998), potentially released from clathrates in Martian permafrost. The greenhouse effect would be short-lived, persisting just long enough for temporary warm-climate effects, such as liquid-water lakes and precipitation that form valleys and upland glaciers. Using a Martian atmosphere computer model (Haberle et al., 1994), calculations show that adding 1–2 bar CO_2 to Mars' atmosphere late in its history would increase mean planetary temperatures to near water's freezing point for roughly 10^7–10^8 years (Gulick et al., 1997). More recently, Schmidt et al. (2022) demonstrated that the Martian ocean at 3 Ga during the Hesperian Period could have been stable by using an advanced general circulation model (GCM). These results suggest that the pressure was sufficient for water to flow on Mars in the time when the floods associated with Hebrus Valles were active.

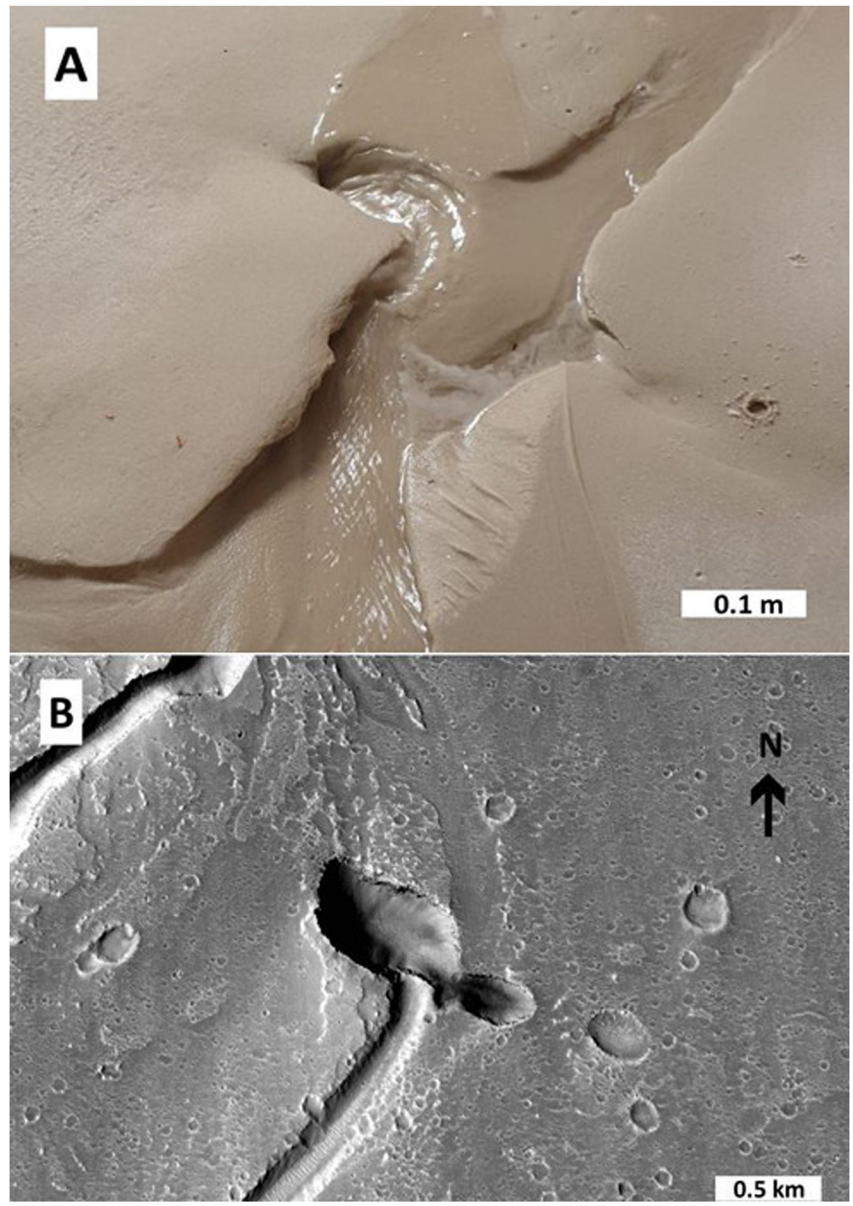

Figure 10. (a) Laboratory simulation of an underground cavernous system within a medium simulating water-saturated subsoil (Exp. 1) (b) sinkhole formation along one channel from Hebrus Valles. Our laboratory simulation suggests that caves along the Hebrus Valles are preferential conduits through which fluid-sediments are actively captured by the evacuated caverns. Panel B is part of Resolution Stereo Camera (HRSC) image H5140_0000_ND3, situated at Martian coordinates 21.50°N and 125.50°E.

5. Conclusions

Our laboratory simulations replicate the fluvial dynamics observed at the downstream end of Hebrus Valles, a distinctive Martian outflow channel located southeast of Utopia Planitia. Unlike other Martian channels obscured by younger sediments, Hebrus Valles uniquely exposes its terminal features, thereby offering valuable insights into interactions between surface flows and subsurface structures. Our experiments employed buried polygonal tunneling configurations in a sandy matrix to emulate incision features specific to this region. These results, constituting the first lab-based evidence of high-volume fluvial events in Hebrus Valles, specifically capture the abrupt « disappearance » of flood waters into the subsurface. Importantly, the study underscores the role of sinkholes as flood capture mechanisms, facilitating the formation of an interconnected network of subterranean channels. Our experiment demonstrates the ability of conduits to facilitate the conveyance of large flood

discharges. This lends credence to our hypothesis that the porous Martian subsurface allows for efficient fluid movement, leading to functional underground conduits for floodwater routing. Moreover, recent in situ data from the Zhurong rover in southern Utopia Planitia have indicated fluctuating groundwater levels, adding to the hydrological importance of this Martian region (Hamran et al., 2022). Such rheological and geological characteristics of the subsurface make Hebrus Valles a significant focal point for human exploration, as noted by Sharma et al. (2019). Our study provides new insights into the subsurface geology, making Hebrus Valles a more appealing target for human exploration than it was before we conducted this study.

Data Availability Statement

Raw spacecraft data used in this study include HiRISE (McEwen, 2007), CTX (Malin, 2007), and MOLA data (Neumann et al., 2003) archived in NASA's Planetary Data System as well as HRSC data archived by ESA (European Space Agency, 2020). Details about the experimental setup and the data themselves are available via the Zenodo archive (Costard et al., 2023).

Acknowledgments
We thank Karin Lehnigk and an anonymous reviewer for their constructive comments and questions, which substantially improved the quality of our manuscript. The authors are funded by the Programme National de Planétologie (PNP) of Institut National des Sciences de l'Univers (CNRS-INSU, France) and the Centre National d'Etudes Spatiales (CNES, France). We acknowledge the HiRISE Team as well as the HRSC Team for the data provided. We thank Claude Lanoe for building the experiment and Steve Gough from emriver Research and Design for providing the hydraulic equipment.

References

Baker, V. R. (1978). The Spokane flood controversy and the Martian outflow channels. *Science*, *202*(4374), 1249–1256. https://doi.org/10.1126/science.202.4374.1249

Baker, V. R. (1982). *The channels of Mars*. University of Texas Press.

Baker, V. R. (2010). Channeled scablands: A megaflood landscape. In *Geomorphological landscapes of the world* (pp. 21–28). Springer Netherlands. https://doi.org/10.1007/978-90-481-3055-9_3

Baker, V. R., Carr, M. H., Gulick, V. C., Williams, C. R., & Marley, M. S. (1992). Channels and valley networks. In H. H. Kieffer, B. M. Jakosky, C. W. Synder, & M. S. Ž. Matthews (Eds.), *Mars*, (pp. 483–522). University of Arizona Press.

Baker, V. R., Strom, R. G., Gulick, V. C., Kargel, J. S., Komatsu, G., & Kale, V. S. (1991). Ancient oceans, ice sheets and the hydrological cycle on Mars. *Nature*, *352*(6336), 589–594. https://doi.org/10.1038/352589a0

Barlow, N. G., Boyce, J. M., Costard, F. M., Craddock, R. A., Garvin, J. B., Sakimoto, S. E. H., et al. (2000). Standardizing the nomenclature of Martian impact crater ejecta morphologies. *Journal of Geophysical Research: Planets*, *105*(E11), 26733–26738. https://doi.org/10.1029/2000je001258

Bretz, J. H. (1923). The channeled Scablands of the Columbia Plateau. *The Journal of Geology*, *31*(8), 617–649. https://doi.org/10.1086/623053

Bretz, J. H. (1969). The Lake Missoula floods and the channeled Scabland. *The Journal of Geology*, *77*(5), 505–543. https://doi.org/10.1086/627452

Bretz, J. H., Smith, H. T. U., & Neff, G. E. (1956). Channeled Scabland of Washington: New data and interpretations. *Geological Society of America Bulletin*, *67*(8), 957–1049. https://doi.org/10.1130/0016

Buczkowski, D. L., & McGill, G. E. (2002). Topography within circular grabens: Implications for polygon origin, Utopia Planitia, Mars. *Geophysical Research Letters*, *29*(7), 1155. https://doi.org/10.1029/2001GL014100

Buczkowski, D. L., Seelos, K. D., & Cooke, M. L. (2012). Giant polygons and circular graben in western Utopia basin, Mars: Exploring possible formation mechanisms. *Journal of Geophysical Research*, *117*(E8), E08010. https://doi.org/10.1029/2011JE003934

Campbell, B., Carter, L., Phillips, R., Plaut, J., Putzig, N., Safaeinili, A., et al. (2008). SHARAD radar sounding of the Vastitas Borealis Formation in Amazonis Planitia. *Journal of Geophysical Research*, *113*(E12), E12010. https://doi.org/10.1029/2008JE003177

Carr, M. H., & Head, J. W., III. (2003). Oceans on Mars: An assessment of the observational evidence and possible fate. *Journal of Geophysical Research*, *108*(E5), 5042. https://doi.org/10.1029/2002je001963

Carr, M. H., & Schaber, G. G. (1977). Martian permafrost features. *Journal of Geophysical Research*, *82*(28), 4039–4054. https://doi.org/10.1029/JS082i028p04039

Catling, C., Leovy, C. B., Wood, S. E., & Day, M. D. (2012). Does the Vastitas Borealis Formation contain oceanic or volcanic deposits. In *Third conference on early Mars: Geologic, hydrologic, and climatic evolution and the implications for life, 21–25 May 2012, Lake Tahoe, Nevada: LPI contribution no. 1680*. abstract 7031.

Clifford, S. M. (1993). A model for the hydrologic and climatic behavior of water on Mars. *Journal of Geophysical Research*, *98*, 10973–11016. https://doi.org/10.1029/93je00225

Clifford, S. M., & Parker, T. J. (2001). The evolution of the Martian hydrosphere: Implications for the fate of a primordial ocean and the current state of the Northern Plains. *Icarus*, *154*(1), 40–79. https://doi.org/10.1006/icar.2001.6671

Costard, F., Dupeyrat, L., Séjourné, A., Bouchard, F., Fedorov, A., & Saint-Bézar, B. (2021). Retrogressive thaw slumps on ice-rich permafrost under degradation: Results of a large-scale laboratory simulation. *Geophysical Research Letters*, *48*(1), e2020GL091070. https://doi.org/10.1029/2020GL091070

Costard, F., Gautier, E., & Brunstein, D. (2007). Siberian Rivers and Martian outflow channels: An analogy. In M. G. Chapman & I. P. Skilling (Eds.), *The geology of Mars: Evidence from Earth-based analogues* (pp. 279–296). Cambridge University Press.

Costard, F., Rodriguez, J. A. P., Godin, E., Séjourné, A., & Kargel, J. (2023). Deciphering Martian flood infiltration processes at Hebrus Valles: Insights from laboratory experiments and remote sensing observations [Dataset]. Zenodo. https://doi.org/10.5281/zenodo.10423753

Costard, F., Sejourne, A., Kargel, J., & Godin, E. (2016). Modeling and observational occurrences of near-surface drainage in Utopia Planitia, Mars. *Geomorphology*, *275*, 80–89. https://doi.org/10.1016/j.geomorph.2016.09.034

Costard, F. M., & Kargel, J. S. (1995). Outwash plains and Thermokarst on Mars. *Icarus*, *114*(1), 93–112. https://doi.org/10.1006/icar.1995.1046

Esri (Producer). (2021). ArcGIS (version 10.9) [Software]. Environmental Systems Research Institute, Inc. Retrieved from https://enterprise.arcgis.com/en/get-started/10.9/linux/what-s-new-in-arcgis-enterprise.htm

European Space Agency. (2020). MEX-M-HRSC-5-REFDR-MAPPROJECTED [Dataset]. European Space Agency. https://doi.org/10.5270/esa-pm8ptbq

Fortier, D., Allard, M., & Shur, Y. (2007). Observation of rapid drainage system development by thermal erosion of ice wedges on Bylot Island, Canadian Arctic Archipelago. *Permafrost and Periglacial Processes*, *18*(3), 229–243. https://doi.org/10.1002/ppp.595

Godin, E., & Fortier, D. (2012). Geomorphology of a thermo-erosion gully, Bylot Island, Nunavut, Canada. *Canadian Journal of Earth Sciences*, *49*(8), 979–986. https://doi.org/10.1139/e2012-015

Godin, E., Fortier, D., & Coulombe, S. (2014). Effects of thermo-erosion gullying on hydrologic flow networks, discharge and soil loss. *Environmental Research Letters*, *9*(10), 105010. https://doi.org/10.1088/1748-9326/9/10/105010

Gulick, V. C., Tyler, D., McKay, C. P., & Haberle, R. M. (1997). Episodic ocean-induced CO_2 greenhouse on Mars: Implications for fluvial valley formation. *Icarus*, *130*(1), 68–86. https://doi.org/10.1006/icar.1997.5802

Haberle, R. M., Tyler, D., McKay, C. P., & Davis, W. L. (1994). A model for the evolution of CO_2 on Mars. *Icarus*, *109*(1), 102–120. https://doi.org/10.1006/icar.1994.1079

Hamran, S. E., Paige, D. A., Allwood, A., Amundsen, H. E. F., Berger, T., Brovoll, S., et al. (2022). Ground penetrating radar observations of subsurface structures in the floor of Jezero crater, Mars. *Science Advances*, *8*(34). https://doi.org/10.1126/sciadv.abp8564

Head, J. W., III., Hiesinger, H., Ivanov, M., Kreslavsky, M., Pratt, S., & Thomson, B. J. (1999). Possible ancient oceans on Mars: Evidence from Mars orbiter laser altimeter data. *Science*, *286*(5447), 2134–2137. https://doi.org/10.1126/science.286.5447.2134

Hiesinger, H., & Head, J. W., III. (2000). Characteristics and origin of polygonal terrain in southern Utopia Planitia, Mars: Results from Mars orbiter laser altimeter and Mars orbiter camera data. *Journal of Geophysical Research*, *105*(E5), 11999–12022. https://doi.org/10.1029/1999JE001193

Jaumann, R., Neukum, G., Behnke, T., Duxbury, T. C., Eichentopf, K., Flohrer, J., et al. (2007). The high-resolution stereo camera (HRSC) experiment on Mars Express: Instrument aspects and experiment conduct from interplanetary cruise through the nominal mission [Dataset]. Planetary and Space Science, *55*, 928–952. https://doi.org/10.1016/j.pss.2006.12.003

Kasting, J. F., & Brown, L. L. (1998). Setting the stage: The early atmosphere as a source of biogenic compounds. In A. Brack (Ed.), *The molecular origins of life: Assembling the Pieces of the Puzzle* (pp. 35–56). Cambridge University Press.

Kreslavsky, M. A., & Head, J. W. (2002). Mars: Nature and evolution of young latitude-dependent water-ice-rich mantle. *Geophysical Research Letters*, *29*(15), 14-1–14-4. https://doi.org/10.1029/2002GL015392

Leverington, D. W. (2011). A volcanic origin for the outflow channels of Mars: Key evidence and major implications. *Geomorphology*, *132*(3), 51–75. https://doi.org/10.1016/j.geomorph.2011.05.022

Lucchitta, B. K., Ferguson, H. M., & Summers, C. (1986). Sedimentary deposits in the northern lowland plains, Mars. *Journal of Geophysical Research*, *91*(B13), E166–E174. https://doi.org/10.1029/JB091iB13p0E166

Malin, M. C. (2007). MRO Context Camera experiment data record level 0 v1.0 [Dataset]. NASA Planetary Data System. https://doi.org/10.17189/1520266

Mars Channel Working Group. (1983). Channels and valleys on Mars. *Geological Society of America Bulletin*, *94*(9), 1035–1054. https://doi.org/10.1130/0016-7606(1983)94<1035:cavom>2.0.co;2

McEwen, A. (2007). Mars reconnaissance orbiter high resolution imaging science experiment, reduced data record, MRO-M-HIRISE-3-RDR-V1.1 [Dataset]. NASA Planetary Data System. https://doi.org/10.17189/1520303

McGill, G. E., & Hills, L. S. (1992). Origin of giant Martian polygons. *Journal of Geophysical Research*, *97*(E2), 2633–2647. https://doi.org/10.1029/91JE02863

Mouginot, J., Pommerol, A., Kofman, W., Beck, P., Schmitt, B., Herique, A., et al. (2010). The 3–5 MHz reflectivity map of Mars by MARSIS/Mars Express: Implications for the current inventory of subsurface H2O. *Icarus*, *210*(2), 612–625. https://doi.org/10.1016/j.icarus.2010.07.003

Mutch, T. A., Arvidson, R. E., Head, J. W., III., Jones, K. L., & Stephen Saunders, R. (1977). *The geology of Mars* (Vol. x, p. 400). Princeton University Press.

Nerozzi, S., Tober, B., Holt, J. W., & Ortiz, M. (2020). *Reconstructing the geologic history of Hebrus Valles and Hephaestus Fossae, Mars with SHARAD*. American Geophysical Union. Fall Meeting 2020, abstract #P016-0004.

Neumann, G., Zuber, M., & Smith, D. E. (2003). MOLA mission experiment gridded data record [Dataset]. NASA Planetary Data System. https://doi.org/10.17189/1519460

Pardee, J. T. (1942). Unusual currents in glacial lake Missoula, Montana. *Geological Society of America Bulletin*, *53*(11), 1569–1600. https://doi.org/10.1130/GSAB-53-1569

Parker, T. J., Gorsline, D. S., Saunders, R. S., Pieri, D. C., & M Schneeberger, D. (1993). Coastal geomorphology of the Martian northern plains. *Journal of Geophysical Research*, *98*(E6), 11061–11078. https://doi.org/10.1029/93JE00618

Parker, T. J., Saunders, R. S., & Schneeberger, D. M. (1989). Transitional morphology in West Deuteronilus Mensae, Mars—Implications for modification of the lowland upland boundary. *Icarus*, *82*(1), 111–145. https://doi.org/10.1016/0019-1035(89)90027-4

Pechmann, J. C. (1980). The origin of polygonal troughs on the northern plains of Mars. *Icarus*, *42*(2), 185–210. https://doi.org/10.1016/0019-1035(80)90071-8

Rodriguez, J. A. P., Bourke, M., Tanaka, K. L., Miyamoto, H., Kargel, J., Baker, V., et al. (2012). Infiltration of Martian outflow channel floodwaters into lowland cavernous systems. *Geophysical Research Letters*, *39*(22), L22201. https://doi.org/10.1029/2012gl053225

Rodriguez, J. A. P., Kargel, J., Baker, V. R., Gulick, V. C., Berman, D. C., Fairén, A. G., et al. (2015). Martian outflow channels: How did their source aquifers form, and why did they drain so rapidly? *Scientific Reports*, *5*(1), 13404. https://doi.org/10.1038/srep13404

Rodriguez, J. A. P., Sasaki, S., & Miyamoto, H. (2003). Nature and hydrological relevance of the Shalbatana complex underground cavernous system. *Geophysical Research Letters*, *30*(6), 1304. https://doi.org/10.1029/2002gl016547

Sauro, F., Pozzobon, R., Massironi, M., De Berardinis, P., Santagata, T., & De Waele, J. (2020). Lava tubes on Earth, Moon and Mars: A review on their size and morphology revealed by comparative planetology. *Earth-Science Reviews*, *209*, 103288. https://doi.org/10.1016/j.earscirev.2020.103288

Schmidt, F., Way, M., Costard, F., Bouley, S., Séjourné, A., & Aleinov, I. (2022). Circumpolar ocean stability on Mars 3 Gy ago. *Proceedings of the National Academy of Sciences of the United States of America*, *19*, 4. https://doi.org/10.1073/pnas.2112930118

Séjourné, A., Costard, F., Gargani, J., Soare, R. J., & Marmo, C. (2012). Evidence of an eolian ice-rich and stratified permafrost in Utopia Planitia, Mars. *Planetary and Space Science*, *60*(1), 248–254. https://doi.org/10.1016/j.pss.2011.09.004

Sharma, R., Srivastava, N., & Yadav, S. K. (2019). Resource potential and planning for exploration of the Hebrus Valles, Mars. *Research in Astronomy and Astrophysics*, *19*(8), 116. https://doi.org/10.1088/1674-4527/19/8/116

Sharp, R. P., & Malin, M. C. (1975). Channels of Mars. *Geological Society of America Bulletin*, *86*(5), 593–609. https://doi.org/10.1130/0016-7606(1975)86<593:com>2.0.co;2

Skinner, J. A., & Mazzini, A. (2009). Martian mud volcanism: Terrestrial analogs and implications for formational scenarios. *Marine and Petroleum Geology*, *26*(9), 1866–1878. https://doi.org/10.1016/j.marpetgeo.2009.02.006

Stuurman, C. M., Osinski, G. R., Holt, J. W., Levy, J. S., Brothers, T. C., Kerrigan, M., & Campbell, B. A. (2016). SHARAD detection and characterization of subsurface water ice deposits in Utopia Planitia, Mars. *Geophysical Research Letters*, *43*(18), 9484–9491. https://doi.org/10.1002/2016GL070138

Sulcanese, D., Komatsu, G., Ori, G. G., & Rodriguez, J. A. P. (2018). Discovery of potential cave skylights in Hebrus Valles and Hephaestus Fossae, Mars. In *49th lunar and planetary science conference 2018*. LPI Contrib. No. 2083.

Tanaka, K. L. (1997). Sedimentary history and mass flow structures of Chryse and Acidalia Planitiae, Mars. *Journal of Geophysical Research*, *102*(E2), 4131–4149. https://doi.org/10.1029/96JE02862

Tanaka, K. L., Skinner, J. A., Dohm, J. M., Irwin III, R. P., Kolb, E. J, Fortezzo, C. M., et al. (2014). *Geologic map of Mars* (Vol. 3292, p. 43). U.S. Geological Survey Scientific Investigations. scale 1:20.000.000, pamphlet. https://doi.org/10.3133/sim3292

Tanaka, K. L., Skinner, J. A., & Hare, T. M. (2005). *Geologic map of the northern plains of Mars* (p. 2888). US Geological Survey Sci. Inv.

Tanaka, K. L., Skinner, J. A., Hare, T. M., Joyal, T., & Wenker, A. (2003). Resurfacing history of the northern plains of Mars based on geologic mapping of Mars Global Surveyor data. *Journal of Geophysical Research*, *108*(E4), 8043. https://doi.org/10.1029/2002je001908

Warner, N., Gupta, S., Muller, J. P., Kim, J. R., & Lin, S. Y. (2009). A refined chronology of catastrophic outflow events in Ares Vallis, Mars. *Earth and Planetary Science Letters*, *288*(1–2), 58–69. https://doi.org/10.1016/j.epsl.2009.09.008